EPJ Web of Conferences **309**, 02017 (2024) https://doi.org/10.1051/epjconf/202430902017
EOSAM 2024

Subsampling Schemes for Compressive Nearfield Spectroscopy

Dario Siebenkotten, *Manuel* Marschall, and *Bernd* Kästner*

Physikalisch-Technische Bundesanstalt, Abbestraße 2-12, 10587 Berlin, Germany

Abstract. Nearfield spectroscopy is crucial for characterizing micro- and nanostructures and it often requires hyperspectral imaging, where at each spatial point a full spectrum is recorded. Due to its combination with an atomic force microscope, nearfield hyperspectral imaging is serial in nature and results in long acquisition times and stability challenges, also restricting its industrial use. In this work, we employ a subsampling strategy combined with low-rank matrix reconstruction in a commercial nearfield spectroscopy system to significantly shorten measurement acquisition times.

1 Introduction

In conventional spectroscopy the spatial resolution is limited by the diffraction limit. In contrast, scanning probe microscopy methods employing near-field techniques offer a means to surpass this limitation. Applying them for hyperspectral imaging (HSI) is often very challenging because of the slow sequential measurement acquisition. In this paper we discuss compressive nearfield spectroscopy which in theory can drastically reduce data requirements [1, 2]. Typically, these approaches require accessing randomly chosen measurement positions individually, leading to idle routes and positioning delays where no data is collected. As a result, the time savings are less substantial than anticipated. Therefore, we employ a practical subsampling scheme, that collects experimental data along specific paths. This method eliminates idle routes, proving to be feasible and significantly quicker than acquiring equivalent measurements at random locations [3].

2 Scattering-type SNOM

We employ a commercial nearfield spectroscopy system based on the principle of scattering-type scanning nearfield optical microscopy (s-SNOM) [4]. The s-SNOM is capable of spectroscopy by means of an asymmetric Michelson interferometer [5] to perform Fourier transform infrared spectroscopy. The 3D data cube that the measurement produces then consists of x and y as spatial coordinates and the interferometer position z.

3 Low-rank matrix reconstruction

The method of low-rank matrix reconstruction may be applied to a measurement set, composed of spatially distributed spectral data, which should have a structure where the variability in the data can be attributed to a few underlying components. Let $X_{ij}, i = 1, \dots, N_r; j = 1, \dots, N_t$, denote the matrix of measurements, where the rows are the spatial positions of the measurements, and the columns are the interferometer positions. The applicability of this method depends on the assumption that the matrix X contains many singular values close to zero and only a few that are substantially larger, suggesting that the data can be compressed into a lower-dimensional space. Details on the actual reconstruction of the full matrix from a subset of measurements can be found in Ref. [6].

4 Route-sampling strategies

To obtain a subset of measurements, it is important to acknowledge that rapid transitions between measurement points are impractical due to the inherent constraints of mechanical stages, which move at limited acceleration and need time to stabilize at each new position. The issue is illustrated in Fig. 1(a). It shows a path through the data cube spanned by the spatial *x*-*y* coordinates and the interferometer axis. The random selection of measurement points is depicted by voxels (black points). Navigating through the data cube involves moving sequentially from one voxel to another, with each voxel marking a measurement location. The path is visualized in rainbow hues, starting with red and progressing to violet at the end of the trajectory. Some positions on these paths go unmeasured, resulting in inefficient use of measurement time and thus, extended total measurement duration. This issue is now addressed by routing strategies based on 3-D boundary reflection.

Fig. 1(b) illustrates a trajectory following a 3D Lissajous curve, where sampling is continuous. However, the sampling of the interferometer axis is done in a non-equidistant and quasi-random manner, which aligns with the requirements of the reconstruction algorithms. This sampling pattern is highlighted by a dashed line along the interferometer axis in the center, with sampled positions

* Corresponding author: bernd.kaestner@ptb.de

marked as black points. Additionally, the trajectory color changes progressively from red to violet over time, making it easier to follow its path.

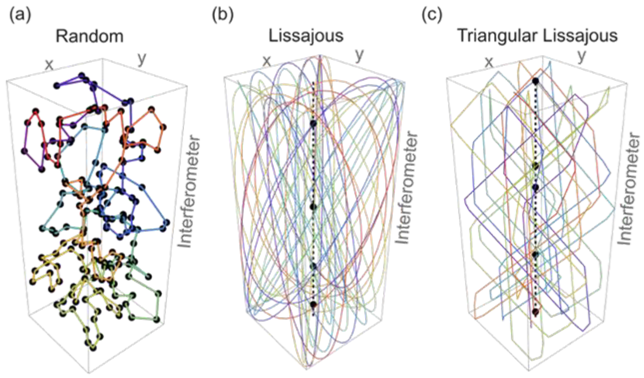

Fig. 1. (a) Measurement route using random sampling, with the path color changing from red to violet to ease tracking. (b) Similar to (a), but with harmonic oscillations in all three axes producing Lissajous curves and continuous measurements. The center is marked by a dashed line and intersections by a black point. (c) Like (b), but with axes moving at constant speeds and reversing at boundaries.

To achieve the target sub-sampling rate throughout the data cube, the oscillation frequencies must be non-commensurate to prevent periodic orbits. However, sinusoidal oscillation tends to concentrate more samples at the map's edges, resulting in a non-uniform sampling pattern. This uneven distribution can result in biased image reconstructions.

To improve the uniformity of sampling while avoiding equidistant intervals along the interferometer axes, a 3D triangle Lissajous sub-sampling scheme has been introduced for spectroscopic laser-scanning imaging, as described in Ref. [7]. This method involves moving at a constant speed in each direction and reversing at the borders. The oscillation frequencies must also be non-commensurate to ensure even filling of the 3D data cube. Fig. 1(c) displays this scheme; the triangular approach achieves more consistent sampling across the data cube, preventing bias in the reconstruction. This is depicted by the quasi-random sampling on the interferometer axes, again marked by the black points on the dashed central line.

5 Application

The method will be employed to various samples such as SiC containing extended triangular defects. The recording time of an HSI map can be reduced by almost an order of magnitude. The possibility of taking homogeneous regions into account will be discussed.

Furthermore, the technique will be utilized on an ultrathin gallium film beneath epitaxial graphene on 6H-SiC, as detailed in Ref. [3] and its cited references. This particular sample presents a challenge due to its heterogeneity and significant spectral variations. Also, in this case the method has been applied successfully, where even with a subsampling rate of 5% reasonable results have been achieved.

We acknowledge financial support by Deutsche Forschungsgemeinschaft (Grants EL 492/1-1, RU 420/13-1, KA 2866/4-1) and within the project 20IND09 PowerElec and 20IND08 MetExSPM from the EMPIR programme co-financed by the Participating States and from the European Union’s Horizon 2020 research and innovation programme.

References

1. B. Kästner, F. Schmähling, A. Hornemann, G. Ulrich, A. Hoehl, M. Kruskopf, K. Pierz, M. B. Raschke, G. Wübbeler, and C. Elster, Opt. Express **26**, 18115 (2018)
2. B. Kästner, M. Marschall, A. Hornemann, S. Metzner, P. Patoka, S. Cortes, G. Wübbeler, A. Hoehl, E. Rühl, and C. Elster, Meas. Sci. Technol., **35**, 015403 (2024)
3. S. Metzner, B. Kästner, M. Marschall, G. Wübbeler, S. Wundrack, A. Bakin, A. Hoehl, E. Rühl, and C. Elster, IEEE Trans. Instrum. Meas., **71**, 1–8 (2022)
4. F. Keilmann and R. Hillenbrand, Phil. Trans. R. Soc. Lond. A, **362,** 787–805 (2004)
5. F. Huth, A. Govyadinov, S. Amarie, W. Nuansing, F. Keilmann, and R. Hillenbrand, Nano Lett., **12,** 3973–8 (2012)
6. M. Marschall, A. Hornemann, G. Wübbeler, A. Hoehl, E. Rühl, B. Kästner, and C. Elster, Opt. Express, **28**, 38762 (2020)
7. H. Lin, C. S. Liao, P. Wang, N. Kong, and J. X. Cheng, Light: Sci. Appl., **7**, 17110–17179 (2018)